International Journal of Pharmacy and Pharmaceutical Sciences

Print ISSN: 2656-0097 | Online ISSN: 0975-1491 Vol 15, Issue 11, 2023

Original Article

DEVELOPMENT, CHARACTERIZATION, AND EVALUATION OF THE ANTIMICROBIAL PROPERTIES OF BIODEGRADABLE POROUS SCAFFOLDS LOADED WITH NATURAL VANILLIN

R. M. AKILA*, M. JANANI

Department of Pharmaceutics, College of Pharmacy, Sri Ramakrishna Institute of Paramedical and Sciences, Coimbatore
Email: akilakathiresan1973@gmail.com

Received: 29 Jul 2023, Revised and Accepted: 27 Sep 2023

ABSTRACT

Objective: The study's objective is to create biodegradable porous scaffolds that are filled with natural vanillin and assess their *in vitro* antibacterial activity**.**

Methods: Scaffolds were fabricated by blending different ratios of chitosan and gelatin along with vanillin using the freeze-drying method. Then the following characterization and evaluation of scaffolds, such as FTIR, SEM, porosity, swelling behaviour, degradation studies, *in vitro* drug release, and antibacterial studies, were carried out.

Results: All of the scaffolds that were created had heterogeneous, well-connected pores and were pale yellow in color. This was validated by SEM, where the porosity is greater than 80% and the mean pore size ranges from 105.25±6.35 µm to 188.58±7.51 µm. With an increase in gelatin concentration, all of the scaffolds showed the maximum water absorption and retention capabilities of 760.15%±4.38% and 664.73%±5.82%. In the 7-day degradation investigation, all samples lost close to 60% of their mass. In the formulation CG11, the vanillin was released gradually over about 96 h. According to the present study, the developed scaffolds CG13-A and CG13-B, as well as CG11-A and CG11-B, displayed a higher zone of inhibition.

Conclusion: Due to its potent antibacterial capabilities, it may be inferred from the current research that vanillin clothed in chitosan-gelatin scaffolds would be a superior option for treating various wound infections, including diabetic wounds.

Keywords: Biodegradable scaffolds, Porous scaffolds, Franz diffusion cell, Chitosan-Gelatin, Natural vanillin

DOI: https://dx.doi.org/10.22159/ijpps.2023v15i11.48987. Journal homepage: https://innovareacademics.in/journals/index.php/ijpps.

INTRODUCTION

A scaffold serves as a temporary framework for the development of cells and tissues. They serve as a platform for cell migration, proliferation, and three-dimensional differentiation, resulting in the development of tissue with properties resembling those of human skin [1]. By offering structural support and a physical setting for cells to attach, develop, migrate, and react to signals, they imitate the extracellular matrix (ECM) [2]. The main tool used to introduce genes, medicines, and cells into the body is a scaffold. "Drug delivery scaffolds" are commonly used to describe porous structures where pharmaceuticals are loaded to achieve high drug loading efficiency and sustained drug release over a longer period of time [3].

The essential requirement for scaffolds is biomaterials as they are designed to interact with biological tissues for augmenting or replacing a native tissue. They must be biocompatible, nonimmunogenic and if desirable, biodegradable; that is a biomaterial should perform safely within the biological environment and any degradation products should be nontoxic [4]. The natural polymers show excellent biocompatibility and biodegradability, low antigenicity. Some polymers have an innate antibacterial and hemostatic activity [5]. Chitosan is one of the most abundant natural amino polysaccharides which is derived from a deacetylated form of native chitin. They show nontoxic, biocompatible and biodegradable characteristics and serve as promising biomaterials for application in biomedical fields such as wound healing, drug delivery, gene delivery and tissue engineering [6]. Chitosan lacks the necessary mechanical strength for tissue engineering; however, this drawback can be solved by blending it with natural polymers like gelatin [7]. By hydrolyzing collagen, gelatin is produced as a protein. Due to their chemical resemblance to the extracellular matrix, they represent interesting materials for the construction of scaffolds. They have strong biocompatibility, biodegradability, low immunogenicity, cost-effectiveness, abundance, and accessible functional groups that permit chemical modification with other biomaterials or biomolecules [8]. The mixture of chitosan and gelatin creates electrostatic interactions between the cationic chitosan and the anionic gelatin molecules. This reduces the electrostatic interaction between the chitosan and the negative charges on the surface of the cell membrane and increases the ability of the cells to migrate across the scaffold. The hydrophilicity of chitosan is increased when gelatin is added, and this hydrophilic surface is appropriate for cell attachment, spreading, and cytoskeleton repair during the process of cell adhesion [9].

A well-known polyphenolic aldehyde called vanillin is generated from mature pods of the *Vanilla Planifolia* orchid. Antimicrobial, antioxidant, anti-inflammatory, antibiotic potentiation and anti-quorum sensing activities have all been documented for vanillin [10]. Therefore, the goal of the study is to create biodegradable scaffolds by mixing various amounts of chitosan, gelatin, and vanillin, then examine their *in vitro* characteristics.

MATERIALS AND METHODS

Materials

From Sigma Aldrich in Mumbai, India, natural vanillin and chitosan were acquired. From Mumbai's Hi Media, gelatin was purchased. In this study, only analytical-grade compounds were employed**.**

Compatibility study of drug and excipients

FTIR studies can be used for determining and assessing the functional groups of various compounds and their compatibility. The dry samples of the drug (vanillin), polymers (chitosan, gelatin), and their physical mixture in a 1:1:1 ratio were taken and observed for analysis to determine the compatibility and interaction between the samples. Samples with a wave number range of 4000–400 cm^{-1} had been used. By determining the presence or absence of IR peaks, the compatibility of the samples was determined.

Formulation of vanillin-loaded porous scaffolds

By using the freeze-drying technique, vanillin-loaded scaffolds were made. 1 g of chitosan was dissolved after being mixed with

100 ml of 1% aqueous acetic acid using a mechanical stirrer. A 10% gelatin solution was made by dissolving 10g of gelatin in 100 ml of hot water. The chitosan solution was subsequently diluted and combined with the gelatin solution in a variety of proportions and strengths, as shown in table 1. The resulting solution was mixed under a magnetic stirrer at a lower rpm until an opaque solution was formed. The medication vanillin was added to the above mixture and stirred for around ten minutes in order to spread the ingredients uniformly. The solution was poured in to the moulds, frozen at-80 °C for two days, and then lyophilized. The resulting scaffolds were then preserved in desiccators for later analysis [11, 12].

Table 1: Formulation of chitosan gelatin scaffolds

Formulation code	Blending ratio of chitosan: gelatin	Vanillin dose
CG31-A	3: 1	200
CG31-B	3: 1	400
CG11-A	1: 1	200
CG11-B	1: 1	400
CG13-A	1: 3	200
CG13-B	1: 3	400

Characterization

Physical appearance

All the prepared scaffolds were visually inspected for colour, surface texture and mechanical strength.

Matrix morphology

The shape and structure of the scaffold was studied under a scanning electron microscope. For surface observation, a small layer of gold was applied to the freeze-dried scaffolds (5 x 5 mm). The working voltage used for the scaffold photography ranged from 8 to 10 kV. Pore morphology and microstructure were assessed [13].

Porosity measurement

The liquid displacement method was used to determine the scaffolds' porosity. Absolute ethanol was employed as the displacement liquid in this procedure. The scaffold was immersed in a graduated cylinder that holds a known volume (V1) of ethanol. Without applying any pressure, the samples were allowed to saturate themselves. After samples had reached saturation, the amount of ethanol that had been injected into the scaffolds was taken into account (V2). The ethanol-impregnated scaffolds were taken out of the cylinder, and the remaining liquid volume was noted as V3. Equation (1) was used to get the scaffolds' porosity percentage (%) [14].

$$\%\Psi = \frac{(V1-V3)}{(V2-V3)} \times 100 \quad \ldots\ldots\ldots\ldots (1)$$

Water absorption and retention capacity

Dry scaffolds of known weight (Wd) were immersed in phosphate-buffered saline (PBS), pH 7.4, at 37 °C for 24 h in order to assess the swelling and water retention capacity of the scaffolds. The samples were then removed, put on filter paper to catch any surface water, and weighed once more (Ww). The obtained scaffolds were centrifuged for three minutes at 500 rpm, and their weights (W'w) were noted. Equations (2 and 3) were used to determine the swelling ratio and water retention of scaffolds [14].

$$\text{Swelling } \% = \frac{(Ww-Wd)}{Wd} \times 100 \quad \ldots\ldots\ldots\ldots\ldots (2)$$

$$\text{Water retaining } \% = \frac{(W'w-Wd)}{Wd} \times 100 \quad \ldots\ldots\ldots\ldots\ldots (3)$$

Degradation test

The scaffolds of size 10 x 10 mm were immersed in phosphate-buffered saline (PBS) pH 7.4 and incubated at 37 °C for 28 d, with the buffer being changed every three days. The samples were weighed on days 3, 7, 14, 21, and 28. The percentage degradation (DP%) was expressed as the percentage degradation of the sample weight from the original weight using equation (4) [14].

$$\text{DP } \% = \frac{(Wd-Wt)}{Wd} \times 100 \quad \ldots\ldots\ldots\ldots (4)$$

Where,

W_t-Final weight scaffold samples.

W_d–Weight of dry scaffolds samples.

***In vitro* drug release study**

The release of vanillin from prepared scaffolds was carried out using a self-fabricated Franz diffusion cell apparatus with a diffusion area of 13.84 cm^2. The Franz diffusion cells consist of donor (for placing the formulation) and receptor (for collecting drug samples) compartments. The diffusion cell consists of a sampling port and a temperature-maintained jacket. The receptor compartment was filled with phosphate-buffered saline, pH 7.4, and it was stirred magnetically by placing a small magnetic bead. Between the donor and receptor compartments of the diffusion cell, the synthetic cellophane membrane was placed.

The formulated scaffolds were cut into a size of 2.1 cm radius and placed over the drug release membrane in such a way that the drug-releasing surfaces face towards the receptor compartment. The donor cell was fixed using clips. The whole assembly was fixed on the magnetic stirrer using magnetic beads at 300 to 400 rpm and maintained at 37±0.5 °C by circulating the constant temperature water through the outer jacket of the diffusion cells. 1 ml of the receptor solution was withdrawn at different time intervals over 96 h. The receptor phase was replenished with an equal volume of phosphate-buffered saline, pH 7.4, at each sample withdrawal. The samples were analysed spectrophotometrically at 231 nm using phosphate-buffered saline pH 7.4 as a blank. The cumulative percentage of drug permeated per square centimeter of scaffolds at various time intervals was calculated and plotted against time [15].

***In vitro* release kinetics**

Using a Microsoft Office Excel Add-In, the drug release kinetics of a vanillin-loaded scaffold were estimated. In order to evaluate the kinetic modelling of drug release, the *In vitro* drug permeation data of the obtained formulation were fitted to zero-order kinetics, first-order kinetics, and the Higuchi model (cumulative percentage of drug release versus log time). The model with a higher correlation coefficient (i.e., higher R^2) was considered to be the best-fit model.

***In vitro* antibacterial activity**

The antibacterial activity of the scaffolds was evaluated using the disc diffusion method with amoxicillin as the standard. Cultures collected from the National Collection of Industrial Microorganisms (NCIM), Pune, were used to create suspensions of *S. aureus, P. aeruginosa, and E. coli* after an overnight incubation.

In the experiment, sterilized scaffold samples of constant weight and same diameter were used. Zones of inhibition were evaluated after the samples had been cultured for an overnight period on a nutrient agar plate with an evenly dispersed bacterial suspension [16].

RESULTS AND DISCUSSION

Compatibility study of drug and excipients

In the present study, a physical mixture of Vanillin in solid form along with different polymers was prepared and analysed by FTIR to find

out the compatibility between the drug and polymers. The vanillin showed a prominent peak at 3023.52 cm-1 for the alcohol group (-OH) and 3312.86 cm-1 for the alkaline group. The peak at 1667.70 cm-1 indicates the presence of alkene group C=C. The alkyl and phenyl groups (C-O) show peaks at 1124.54 cm-1, 1153.47 cm-1, 1200.73 cm-1, 1266.31 cm-1. The FTIR spectrum of chitosan–gelatin and vanillin shows prominent peaks at 3167.22 cm-1 for hydroxyl stretching and 2900.94 cm-1 for asymmetrical CH stretching in the methylene group. The absorption bands obtained at 1667.52 cm-1 and 1463.97 cm-1 are characteristic of C=N stretching vibration and C=C stretching due to aromatic rings, respectively. The distinctive absorption bands appearing at 1266.31 cm-1, 1124.54 cm-1, 1028.09 cm-1, 893.07 cm-1 and 732.97 cm-1 were assigned to the C-O stretching in phenol, C-O-C linkage, alcoholic C-O stretching, C-H deformation, and C-H out of plane bending in aromatic compounds, respectively.

The unique peak of the chitosan-gelatin at various concentrations resembled that of the parent molecules. Due to the presence of gelatin, the chitosan-gelatin showed intense peaks at 897 and 607 cm-1; depending on the amount of gelatin, this intensity might rise or decrease. The-C=O and amino II absorption bands, which are located at 1667.54 cm-1 and 1590.36 cm-1, respectively, changed to a lower wave number as the gelatin concentration increased. These alterations revealed that the development of the polyelectrolyte complex involved chemical interactions between the chains of the molecules of chitosan and gelatin as well as intermolecular hydrogen bonds between chitosan and gelatin molecules. This might be connected to the fact that chitosan and gelatin formed an interpenetrating polymeric network without significantly altering their chemical characteristics. Furthermore, it appears that chitosan works with gelatin to connect them together in the composite scaffold by offering a place for gelatin to anchor. In light of this, there were no abnormal peaks observed in the IR spectra of the drugs and excipients (fig. 1-2).

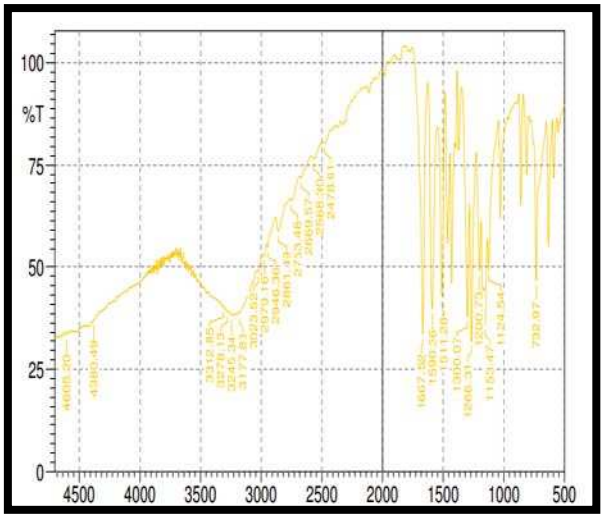

Fig. 1: FTIR spectra of vanillin

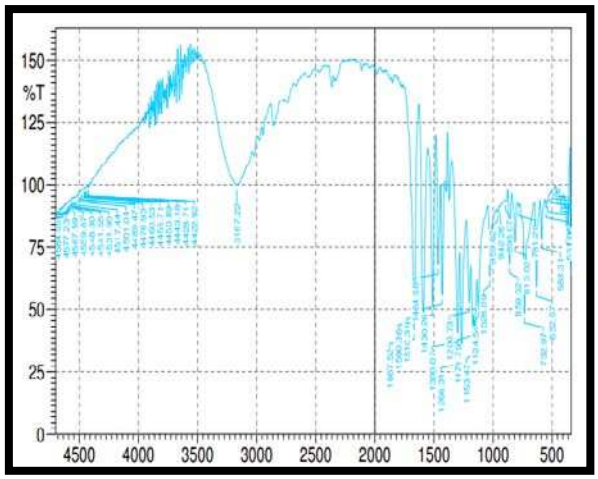

Fig. 2: FTIR peak of chitosan–gelatin–vanillin

Physical appearance

The scaffolds that were all created were opaque and pale yellow. The formulation, CG31, had a weak mechanical strength and a surface that was extremely porous. The CG11 scaffold showed excellent mechanical properties and was very porous with a spongy feel. Due to surface cracking and inefficient drying, the formulation CG13 exhibited an unfavorable physical appearance (fig. 3-5). The formulation has not changed significantly despite the vanillin dose being increased.

Fig. 3

Fig. 4

Fig. 5

Fig. 3-5: Formulated scaffolds with different concentrations of Chitosan (C) and Gelatin (G) (CG31, CG11 and CG13)

Table 2: Mean pore size of scaffolds

Cf Formulation umn1	Minimum pore size	Maximum pore size
CG31	105.25±6.35	188.58±32.51
CG11	119.43±1.84	159.49±28.54
CG13	113.61±2.84	150.25±41.59

Data are expressed as mean±SD (n=3)

Matrix morphology

For cell penetration and multiplication, the right pore size was necessary. A crucial component for the exchange of gas, waste, and nutrients for cells inside the scaffolds, all of the samples included diverse and linked open pores. Using Image J software, the SEM images (fig. 6-8) were processed, and the results showed that the sample's pore size ranged from 105 µm to 188 µm. Table 2 lists the

scaffolds minimum and maximum pore diameters. Due to the increased concentration of chitosan in formulation CG31-A, the pore size was the biggest at 188 µm, which is consistent with the study done by Azizian *et al.* (2018) [13]. The hydrophilic nature of chitosan and gelatin, which encourages the absorption of higher water contents and results in the creation of larger ice crystals that were evaporated during the lyophilization process and observed as pores, may also be the reason why all the scaffolds have larger pores.

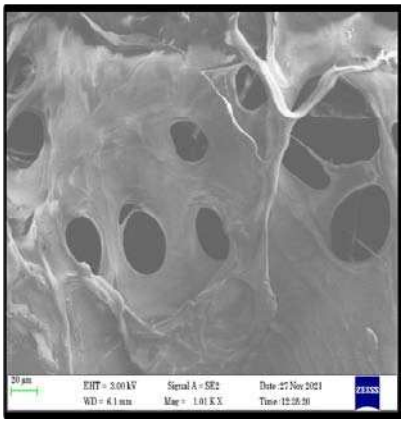

Fig. 6: SEM of CG31

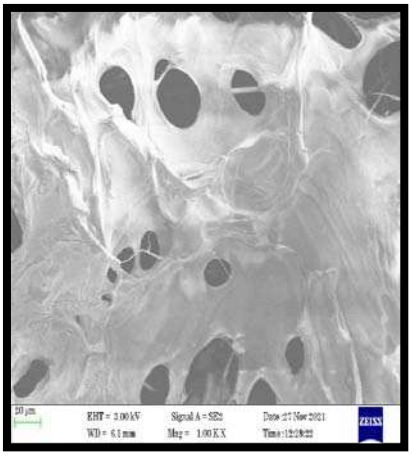

Fig. 7: SEM of CG11

Porosity measurement

The characteristic of porosity is crucial for tissue engineering scaffolds. Scaffolds need to have the right amount of porosity for cell growth and nutrient gas exchange [17]. Table 3 displays the scaffolds porosity %. Due to the bigger holes in the formulation CG31, it had the maximum porosity, which decreased as the amount of gelatin in the formulation increased. These chitosan gelatin scaffolds were found to be suitably porous, allowing for a simple exchange of nutrients and metabolic waste as well as a significant interior surface area for cell adhesion and migration. It was underlined by Irina et al. (2020) that scaffolds having porosity between 60 and 90% are ideal for wound dressing, and all the formulated scaffolds have met this criterion and are good candidates for wound dressing [18].

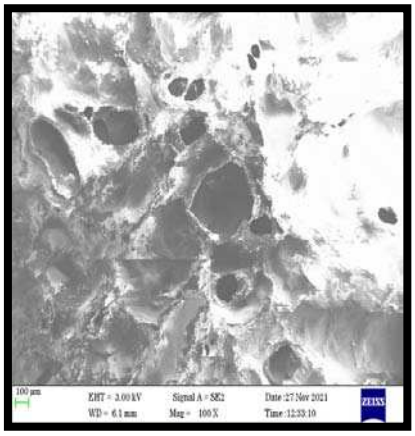

Fig. 8: SEM of CG13

Table 3: Porosity percentage of scaffolds

Scaffolds	Porosity percentage
CG31–A	90.56%±1.2 %
CG31–B	91.23 %±1.65%
CG11–A	86.09 %±1.04 %
CG11–B	87.43 %±0.66 %
CG13–A	81.45 %±1.06 %
CG13-B	83.56 %±1.17 %

Data were expressed as mean±SD (n=3)

Water absorption and retention capacity

The ability to absorb wound exudates is a necessary quality in a wound dressing material. This helps with the movement of cellular nutrients, the secretion of excessive amounts of bodily fluid during the healing process, the preservation of extracellular space, and tissue hydration. Scaffolds' interior pores, both big and small, are easily able to take in water. These scaffolds have a very high swelling capacity and the potential to retain more water than their original weight, according to the swelling investigations done on them (table 4). These findings suggested that all types of scaffolds can create an environment that is suitable by absorbing and holding onto large amounts of water. Due to the increased gelatin concentration, CG13A and CG13B showed the highest swelling capacity. Since polar peptides are found in gelatin and chitosan has a high water absorption capacity, the samples swelled by more than 500%. The scaffold structure might, however, become more floppy as a result, making it easier to extend the system's macromolecular strands.

Table 4: Water absorption and water retention capacity of scaffolds

Scaffolds	Water absorption capacity	Water retention capacity
CG31–A	547.94 %±6.15 %	429.41 %±2.64 %
CG31–B	550.62 %±3.29 %	431.09 %±3.76 %
CG11–A	718.18 %±2.42 %	627.27 %±2.92 %
CG11–B	721.71 %±1.35 %	631.46 %±2.94 %
CG13–A	757.14 %±2.85 %	661.98 %±3.74 %
CG13-B	760.15 %±4.38 %	664.73 %±5.82 %

Data were expressed as mean±SD (n=3)

Degradation test

Scaffolds should biodegrade and bio-resorb at a rate that is consistent with the growth of new tissue at the wound site. The controlled degradation behavior of scaffolds in wound environments plays an important role in the regeneration of new tissues. An investigation on the *in vitro* degradation of gelatin and chitosan scaffolds in PBS at 37 °C could determine their long-term reliability, resorbability, and mechanical stability. The rate of degradation in PBS solutions considerably increased with an increase in the gelatin content. Three days of incubation resulted in a significant mass reduction in all of the scaffolds. Due to the increased gelatin concentration, the samples CG13-A and CG13-B exhibited the highest levels of deterioration (fig. 9). The sample CG31 indicated a decrease in mass loss and the lowest rate of degradation. It's possible that this variation is brought on by changes in the structure's hydrophilic group density [19]. The shape of scaffolds is influenced by surface area because a higher surface area causes more water molecules to diffuse into the structure.

The scaffolds rate of degradation is crucial because if they disintegrate rapidly, like CG13-A and CG13-B, the cells cannot adhere to them, divide, or proliferate. To restore tissue functions, it is ideal for cells to be deposited in the ECM when the scaffolds degrade.

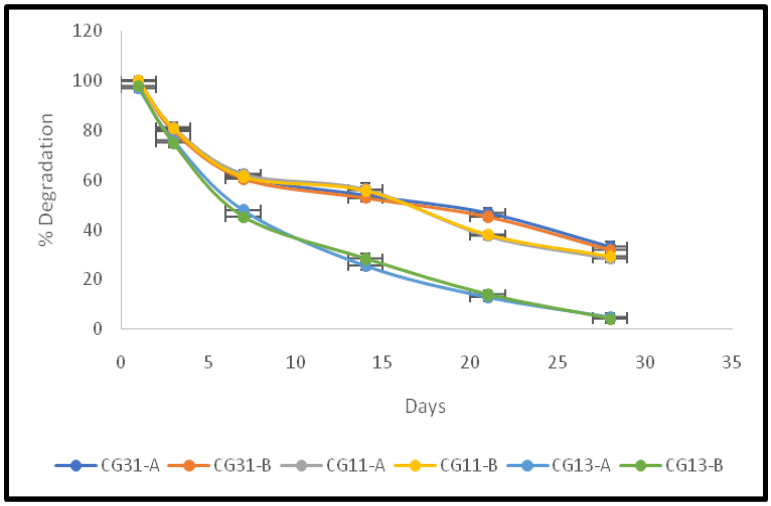

Fig. 9: Degradation rate of vanillin loaded chitosan–gelatin scaffolds CG31-A and CG31-B, the data were expressed as mean±SD (n = 3)

***In vitro* drug release study**

Because of their hydrophilic character, the scaffolds with a high concentration of gelatin (CG13-A, B) released drugs more quickly than other formulations. One of the key factors that regulates the release of the loaded pharmaceuticals is the hydrophilicity of the drug delivery mechanism. Therefore, gelatin's hydrophilicity encourages quick disintegration into the release media, which can eventually result in increased water molecule penetration into the scaffold's core and quick vanillin diffusion. In contrast, the scaffolds made with high chitosan concentrations (CG31-A and B) had a slow-release profile because chitosan has low solubility and slows down drug release. Chitosan and gelatin (CG11-A and B) at equal amounts can effectively regulate the drug release rate. This may be explained by the fact that a lower concentration of gelatin leads to less scaffold degradation, which in turn results in less release medium penetrating the matrix and lowering drug release. On the other hand, a decrease in chitosan content limits the amount of water that may enter the scaffolds, which leads to a controlled release of drugs from the scaffold matrix. A small portion of weakly bound vanillin that releases when it comes into touch with the release medium may be the cause of the initial burst release of vanillin. Vanillin is trapped in porous scaffolds, which causes its continuous release due to the combined effects of vanillin and chitosan interactions [20]. According to some reports, vanillin and gelatin interact through hydrogen bonds, electrostatic interactions, and hydrophobic interactions. Chitosan and the vanillin aldehyde group can also react with one another via the Schiff base reaction (fig. 10-12).

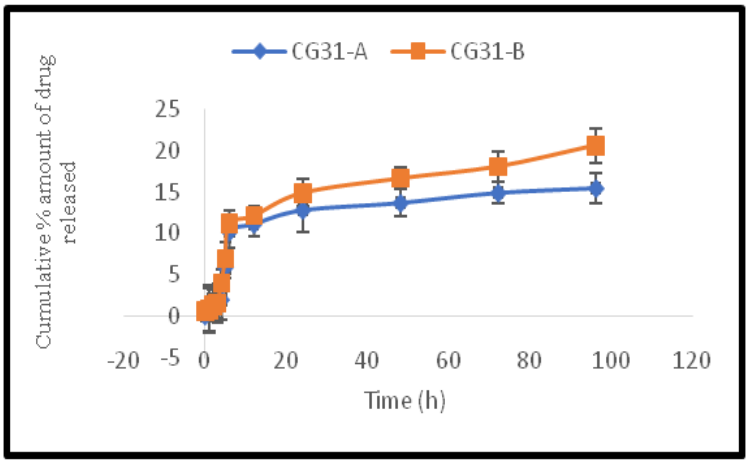

Fig. 10: Percentage drug release of scaffold CG31, the data were expressed as mean±SD (n = 3)

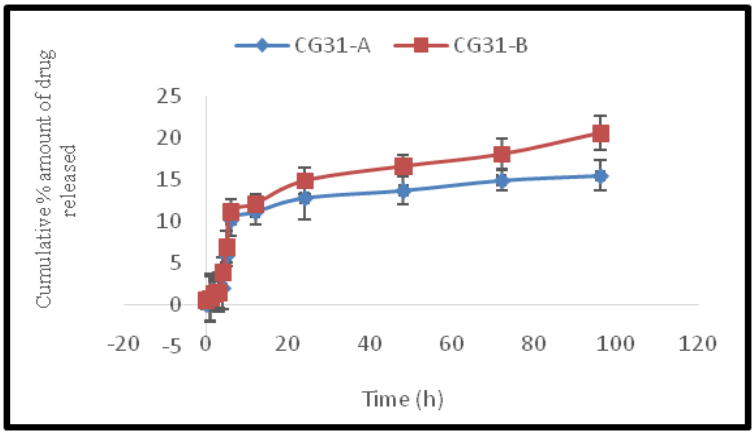

Fig. 11: Percentage drug release of scaffold CG11, the data were expressed as mean±SD (n = 3)

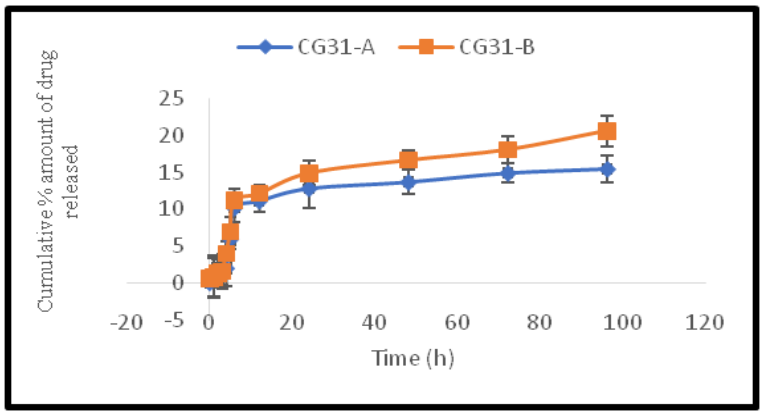

Fig. 12: Percentage drug release of scaffold CG13, the data were expressed as mean±SD (n = 3)

Table 5: Different kinetic models applied on release behaviour of vanillin from scaffolds

Formulation code	Regression constant value (R^2)				
	Zero-order	First order	Higuchi's model	Korsemeyer Peppas model	Hixson crowell
CG31-A	0.7635	0.7547	0.5571	0.618	0.7588
CG31-B	0.8241	0.8128	0.611	0.6871	0.8176
CG11-A	0.9497	0.8688	0.7748	0.8544	0.9009
CG11-B	0.9634	0.8951	0.7965	0.8752	0.9228
CG13-A	0.9366	0.9159	0.889	0.8473	0.9289
CG13-B	0.9467	0.9004	0.8927	0.8359	0.9163

***In vitro* release kinetics**

Several studies on the drug release kinetics were conducted on the *in vitro* release characteristics of formulations. It was discovered that the release profile for the formulations obeyed that specific kinetics and displayed maximum R2 values. As can be seen from the data, zero-order plots have a regression coefficient value that is more closely related to unity. The release of drugs from scaffolds thus appears to follow zero-order kinetics.

***In vitro* antibacterial activity**

By using the disc diffusion method, the *in vitro* antibacterial activity of vanillin-loaded chitosan/gelatin scaffolds was investigated against *Staphylococcus aureus, Pseudomonas aeruginosa, and Escherichia coli.* These organisms were chosen as a pathogenic bacterial model for *in vitro* antibacterial activity since they are frequently detected in diabetic wounds [21].

These findings imply that under the investigated conditions, all scaffolds demonstrated antibacterial inhibitory efficacy. Due to the synergistic antibacterial activity of chitosan and vanillin, the scaffolds CG31-A and CG31-B had shown better efficacy than the rest of the formulation. When compared to *Pseudomonas aeruginosa* and *Escherichia coli,* the scaffold had significantly greater efficacy against *Staphylococcus aureus* strains (table 6) (fig. 13-15). Our results on the antibacterial properties of vanillin are consistent with a prior study that used vanillin added to calcium phosphate powders. The scaffolds that are vanillin-loaded, therefore, have potential as antibacterial wound dressings.

Table 6: Comparative zone of inhibitions of composite scaffolds against *Staphylococcus aureus*, *Pseudomonas aeruginosa* and *Escheria coli*

Organisms	CG31-A	CG31-B	CG11-A	CG11-B	CG13-A	CG13-B	STD
E. coli	13±1.29	15±3.26	10±1.37	13±1.27	1±2.17	6±3.28	20±2.17
Pseudomonas aeruginosa	12±2.32	13±2.24	11±1.16	14±2.33	1±3.13	6±3.21	20.5±2.89
Staphylococcus aureus	16±3.28	17±2.08	14±2.39	16±3.16	1±3.16	5±3.16	20±3.17

The data were expressed as mean±SD (n = 3).

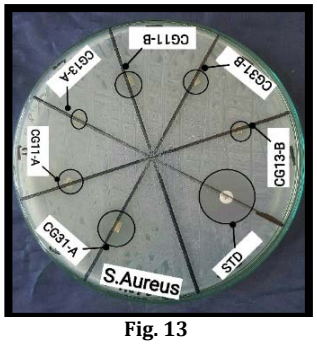

Fig. 13

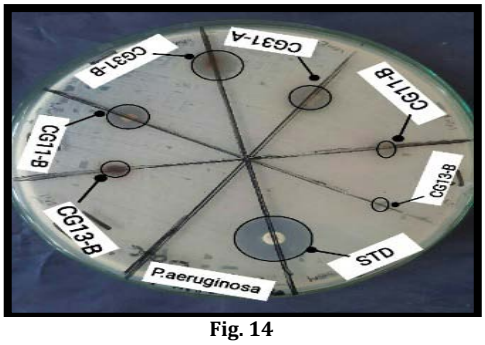

Fig. 14

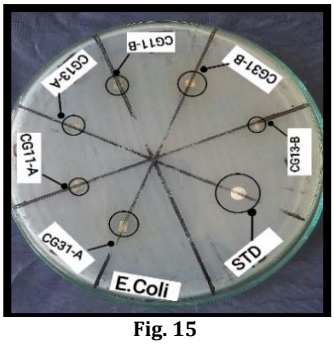

Fig. 15

Fig. 13-15: Zone of inhibition of different scaffold against *Staphylococcus aureus, Pseudomonas aeruginosa and Escherichia coli* respectively

CONCLUSION

Using freeze-drying, vanillin-loaded gelatin and chitosan-based biodegradable scaffolds were developed. Pore diameters less than 200 µm were present in all the synthesized scaffolds, which featured pores that were both heterogeneous and well-connected. Regarding mechanical strength, swelling, porosity, biodegradation, and biocompatibility, these scaffolds met the criteria for the optimum supporting structure. In order to sustain the release of vanillin and reduce infection, CG11 scaffolds served as a matrix. The formulation was not significantly impacted by the vanillin dose variation; however, its antibacterial property increased as the dose was increased. It is possible to draw the conclusion that vanillin-based scaffolds could be a promising choice for a diabetic wound dressing based on the results of the current research. For their validity to be established, additional animal and human investigations are required.

FUNDING

Nil

AUTHORS CONTRIBUTIONS

Both authors have contributed equally.

CONFLICT OF INTERESTS

The authors declare that there is no conflict of interests regarding the publication of this paper.

REFERENCES

1. Ninan N, Muthiah M, Park IK, Wong TW, Thomas S, Grohens Y. Natural polymer/inorganic material based hybrid scaffolds for skin wound healing. Polym Rev. 2015 Jul 3;55(3):453-90. doi: 10.1080/15583724.2015.1019135.
2. Chan BP, Leong KW. Scaffolding in tissue engineering: general approaches and tissue-specific considerations. Eur Spine J. 2008 Dec;17(4)Suppl 4:467-79. doi: 10.1007/s00586-008-0745-3, PMID 19005702.
3. Garg T, Singh O, Arora S, Murthy RS. Scaffold: a novel carrier for cell and drug delivery. Crit Rev Ther Drug Carrier Syst. 2012;29(1):1-63. doi: 10.1615/critrevtherdrugcarriersyst.v29.i1.10, PMID 22356721.
4. Di Gregorio Madeleine M. Scaffold design considerations for soft tissue regeneration [electronic thesis] and Dissertation Repository; 2019. p. 6532. Available from: http://ir.lib.uwo.ca/etd/6532.
5. Blanco Fernandez B, Castano O, Mateos Timoneda MA, Engel E, Perez Amodio S. Nanotechnology approaches in chronic wound healing. Adv Wound Care. 2021 May 1;10(5):234-56. doi: 10.1089/wound.2019.1094, PMID 32320364.
6. Manasa MT, Ramanamurthy KV, Bhupathi PA. Electrospun nanofibrous wound dressings: a review on chitosan composite nanofibers as potential wound dressings. Int J App Pharm. 2023. Jul;15(4):1-11. doi: 10.22159/ijap.2023v15i4.47912.
7. Calori IR, Braga G, de Jesus PdCC, Bi H, Tedesco AC. Polymer scaffolds as drug delivery systems. Eur Polym J. 2020 Apr 15;129:109621. doi: 10.1016/j.eurpolymj.2020.109621.
8. Afewerki S, Sheikhi A, Kannan S, Ahadian S, Khademhosseini A. Gelatin-polysaccharide composite scaffolds for 3D cell culture and tissue engineering: towards natural therapeutics. Bioeng Transl Med. 2019 Jan;4(1):96-115. doi: 10.1002/btm2.10124, PMID 30680322.
9. Jafari J, Emami SH, Samadikuchaksaraei A, Bahar MA, Gorjipour F. Electrospun chitosan-gelatin nanofiberous scaffold: fabrication and *in vitro* evaluation. Biomed Mater Eng. 2011 Jan 1;21(2):99-112. doi: 10.3233/BME-2011-0660, PMID 21654066.
10. Arya SS, Rookes JE, Cahill DM, Lenka SK. Vanillin: a review on the therapeutic prospects of a popular flavouring molecule. Adv Tradit Med (ADTM). 2021 Sep;21(3):1-17. doi: 10.1007/s13596-020-00531-w.
11. Nguyen VC, Nguyen VB, Hsieh MF. Curcumin-loaded chitosan/gelatin composite sponge for wound healing application. Int J Polym Sci. 2013. doi: 10.1155/2013/106570.
12. Indrani DJ, Budiyanto E, Hayun Hayun. Preparation and characterization of porous hydroxyapatite and alginate composite scaffolds for bone tissue engineering. Int J App Pharm. 2017. Dec;9(2):98-102. doi: 10.22159/ijap.2017.v9s2.24.
13. Nokoorani YD, Shamloo A, Bahadoran M, Moravvej H. Fabrication and characterization of scaffolds containing different amounts of allantoin for skin tissue engineering. Sci Rep. 2021 Aug 9;11(1):16164. doi: 10.1038/s41598-021-95763-4, PMID 34373593.
14. Sanchez Cardona Y, Echeverri Cuartas CE, Lopez MEL, Moreno Castellanos N. Chitosan/gelatin/pva scaffolds for beta pancreatic cell culture. Polymers. 2021 Jul;13(14):2372. doi: 10.3390/polym13142372, PMID 34301129.
15. Azizian S, Hadjizadeh A, Niknejad H. Chitosan-gelatin porous scaffold incorporated with chitosan nanoparticles for growth factor delivery in tissue engineering. Carbohydr Polym. 2018 Dec 15;202:315-22. doi: 10.1016/j.carbpol.2018.07.023, PMID 30287006.
16. Zabad IEM, Amin MN, El-Shishtawy MM. Protective effect of vanillin on diabetic nephropathy by decreasing advanced glycation end products in rats. Life Sci. 2019 Dec 15;239:117088. doi: 10.1016/j.lfs.2019.117088, PMID 31759039.
17. She Z, Jin C, Huang Z, Zhang B, Feng Q, Xu Y. Silk fibroin/chitosan scaffold: preparation, characterization, and culture with HepG2 cell. J Mater Sci Mater Med. 2008 Dec;19(12):3545-53. doi: 10.1007/s10856-008-3526-y, PMID 18622765.
18. Negut I, Dorcioman G, Grumezescu V. Scaffolds for wound healing applications. Polymers (Basel). 2020 Sep;12(9):2010. doi: 10.3390/polym12092010, PMID 32899245.
19. Lee SB, Kim YH, Chong MS, Hong SH, Lee YM. Study of gelatin-containing artificial skin V: Fabrication of gelatin scaffolds using a salt-leaching method. Biomaterials. 2005 May;26(14):1961-8. doi: 10.1016/j.biomaterials.2004.06.032, PMID 15576170.
20. Tomadoni B, Ponce A, Pereda M, Ansorena MR. Vanillin as a natural cross-linking agent in chitosan-based films: optimizing formulation by response surface methodology. Polym Test. 2019 Sep;78:105935. doi: 10.1016/j.polymertesting.2019.105935.
21. Banu A, Noorul Hassan MM, Rajkumar J, Srinivasa S. Spectrum of bacteria associated with diabetic foot ulcer and biofilm formation: a prospective study. Australas Med J. 2015 Sep 30;8(9):280-5. doi: 10.4066/AMJ.2015.2422, PMID 26464584.